*Progress In Electromagnetics Research Letters, Vol. 16, 181–190, 2010*

# WIDEBAND RECTANGULAR DIELECTRIC RESONATOR ANTENNA (DRA) WITH SLOT-FED DESIGN

**Z. Weng, X. Wang, Y. Jiao, and F. Zhang**

National Laboratory of Antennas and Microwave Technology
Xidian University
Xi'an, Shaanxi 710071, China

**Abstract**—A novel wideband rectangular dielectric resonator antenna (DRA) is proposed in this paper. A hybrid structure with an isolated dielectric resonator (DR) and an equivalent air-dielectric DR is introduced by lifting the resonator from the ground plane. The hybrid structure is excited by a slot-fed mechanism to obtain a smooth transition between each resonant mode. The resonant modes of the isolated DR and the equivalent DR are merged together to form a wideband impedance bandwidth. It is found that the bandwidth of the proposed antenna can be greatly enhanced by using the hybrid DRA structure instead of the case mounted on the ground plane. A detailed parametric study is carried out to analyze the characteristics of the proposed antenna. Measured results show that the proposed DRA has a 10 dB impedance bandwidth of 61% from 2.4 GHz to 4.5 GHz and the radiation pattern is stable through the operating frequency.

## 1. INTRODUCTION

Dielectric resonator antennas (DRAs) have received lots of attention since they were introduced in the mid-1980s due to several attractive characteristics [1–19]. They are quite useful for high frequency applications, where Ohmic losses tend to be a serious problem for conventional metallic antennas. Additionally, they offer wider bandwidths than microstrip patch antennas that are commonly used at the same frequencies. Many different shaped DRAs have been investigated, such as cylindrical, spherical, and rectangular configurations. Recently, one major aspect of the research on DRAs

*Received 11 June 2010, Accepted 10 August 2010, Scheduled 16 August 2010*
Corresponding author: Z. Weng (zbweng2003@163.com).

has been focused on the bandwidth, and several techniques have been proposed to broaden the bandwidth. One type of these effective methods uses some special composite DR structures [1–3]. For example, stacked dielectric resonators (DRs) with different materials have been studied by Shum in [1], and Kishk et al. have proposed a wideband DRA by using stacked DRs with different materials to obtain multi-resonance operation [2]. After that, Walsh et al. [3] have investigated an embedded stacked DRA and achieved a bandwidth from 2.5 GHz to 4.5 GHz. However, the bandwidth of these proposed antennas is less than 1 : 2 and hard to further enhance the impedance properties while maintaining stable radiation performance. Other configurations of DR can also be used to broaden the bandwidth, such as tetrahedron and triangular [4], L-shaped [5] or T-shaped [6] and so on. Another kind of methods uses special feeding mechanisms [7–11]. The drawback of this kind wideband DRAs is that the radiation pattern is deformed during the operating band.

In this paper, a wideband slot-fed rectangular dielectric resonator antenna is presented. The dielectric resonator is lifted from the ground plane to form an isolated DR and an equivalent air-dielectric DR. It is found that, the bandwidth of the resonant modes can be greatly enhanced by using an air-dielectric DR comparing to the conventional DRA. As a result, a smooth transition from one resonant mode to another can be achieved by using the air-dielectric DR structure and a wide operating bandwidth can be obtained. Parametric studies have been carried out by using CST software to investigate the performances of the proposed DRA. By combining the modes of the DR, a slot-fed DRA with a 10 dB impedance bandwidth of 61% from 2.4 GHz to 4.5 GHz is achieved while maintaining good radiation pattern.

## 2. RESONANT MODES OF RECTANGULAR DRS

The proposed wideband DRA structure is shown in Fig. 1. It consists of a rectangular dielectric resonator and a center slot-fed mechanism which is printed on a substrate of thickness $t = 2\,\text{mm}$ and relative permittivity $\varepsilon_r = 2.65$. The ground plane is printed on the substrate with a dimension of $100 \times 100\,\text{mm}^2$. The rectangular dielectric resonator is centrally placed over the ground with the dimension of $a = b = 28.5\,\text{mm}$, a height of $h = 19.5\,\text{mm}$ and a relative permittivity of $\varepsilon_r = 9.8$. A hexagonal patch is connected to a microstrip feeding line of length $L_3$ and width $W_{50}$. A rectangular slot is etched on the ground plane as a feeding mechanism.

The thickness of the air gap inserted between the DR and the ground plane is denoted by $g$. It is well known that, the value of

the $Q$-factor can be controlled by adjusting the effective dielectric constant [12]. The introduction of this air gap results in a lowering of the effective dielectric constant of the DRA. The bandwidth of the resonant modes can be expanded due to the reducing $Q$-factor [18, 19]. Actually, a lower limit on the value of the dielectric constant is demanded to contain the fields within the dielectric resonator in order to resonate. As a result, a relative permittivity around 10, which is close to the practical lower bound for DR, is chosen for our designs. This hybrid method was first used by Mongia and Ittipiboon in [12] and a summary for $TE^{y}_{mnl}$ modes of the proposed structure is as follows:

$$\begin{aligned} k_y(a/2) &= \tan^{-1}\left(\frac{[k_0^2(\varepsilon_r-1)-k_y^2]^{1/2}}{k_y}\right)+\frac{1}{2}(m-1)\pi \quad m=1,2\ldots \\ k_x &= \frac{n\pi}{b}, \quad n=1,2\ldots \\ k_z &= \frac{l\pi}{2l} \quad l=1,2\ldots \end{aligned} \tag{1}$$

where $k_x$, $k_y$ and $k_z$ represent the mode wave numbers inside the dielectric resonator and subscripts $m$, $n$, and $l$ denote the number of extremes in the $x$, $y$, and $z$ directions, respectively. The mode wave numbers also satisfy the separation equation:

$$f_r = \frac{c}{2\pi\sqrt{\varepsilon_r}}\sqrt{k_x^2+k_y^2+k_z^2} \tag{2}$$

in which $f_r$ is the resonant frequency and $c$ is the wave velocity in the free space.

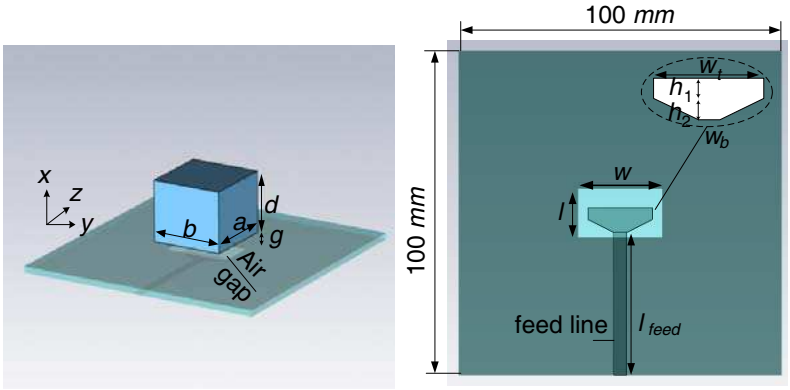


**Figure 1.** Geometry of the proposed DRA.

With reference to Fig. 1, when the DR is lifted from the ground plane, a dual-segment DRA is formed. The air gap inserts serves to transform the impedance of the DRA to that of the slot by concentrating the fields underneath the DRA, this significantly improves the coupling performance. Meanwhile, the introduction of this air space results in a lowering of the effective air-dielectric constant of the DRA, which in turn lowers the $Q$-factor but also increases the resonant frequency. The bandwidth can also be expanded due to the reducing $Q$-factor. To account for the effect of the insert and substrate on the resonant frequency of the dual-segment DRA, the dielectric wave guide model equations are modified by an effective permittivity ($\varepsilon_{eff}$) and effective height ($H_{eff}$). Adopting a simple static capacitance model [7], the effective permittivity of the air-dielectric DRA is calculated using:

$$\varepsilon_{eff} = \left( \frac{d \times \sqrt{\varepsilon_r} + g}{H_{eff}} \right)^2 \tag{3}$$

The effective height $H_{eff}$ is simply the sum of the DRA height $H_{eff} = d + g$.

Additionally, since the dielectric constant of the air is much smaller than the dielectric resonator and the air gap is big enough, the upper dielectric can also be defined as an isolated DR which can contain the fields within the DRA. As a result, the dielectric wave guide model equations are modified by using $k_z = \frac{l\pi}{d}$, $l = 1, 2 \ldots$ to calculate the resonant frequency of the isolated DR. In summary, the resonant modes are defined by the hybrid structure that consists of the effective air-dielectric resonator and the isolated resonator.

## 3. EFFECT OF DRA MODIFICATION

### 3.1. Thickness of the Air Gap

The thickness of the air gap $g$ between the DR and the ground plane plays an important role in the bandwidth enhancement. When the air gap is big enough, the resonant frequencies can be calculated by using Equations (1) and (2). The electrical field distributions of each resonant mode are shown in Fig. 2. The proposed DRA can be considered as a hybrid structure of an effective DR or an isolated DR while resonate at different frequencies. Four resonant modes, effective $TE^y_{111}$ mode, isolated $TE^y_{111}$ mode, effective $TE^y_{113}$ mode and isolated $TE^y_{121}$ mode are observed within the operating bandwidth. Fig. 3 shows the simulated reflection coefficient of the proposed DR with different air gaps ($g$). It can be found that, the first resonant

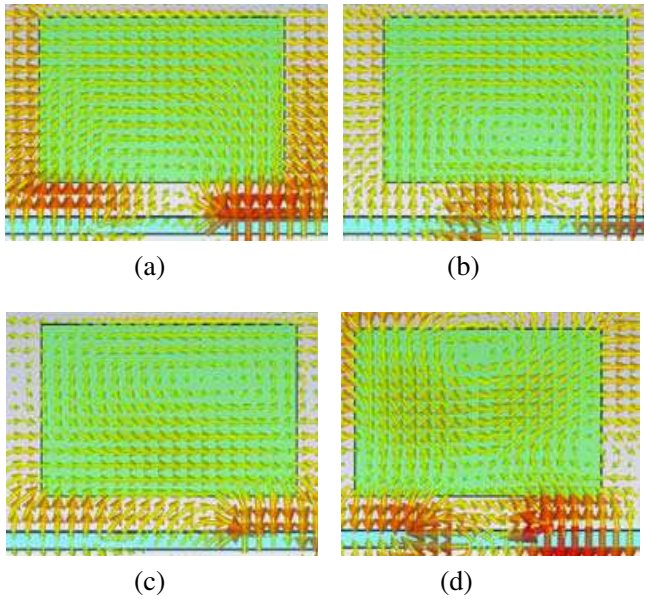


**Figure 2.** Electrical distribution of resonant modes (in the $XZ$ plane). (a) 2.6 GHz, (b)3.17 GHz, (c)3.7 GHz, (d)4.3 GHz.

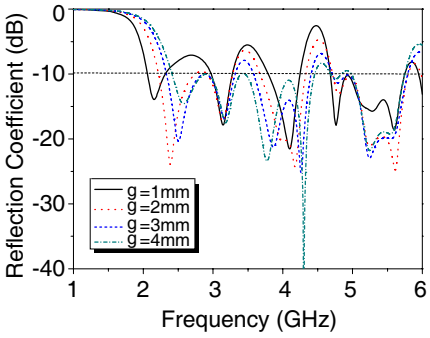


**Figure 3.** Reflection coefficient of the proposed DRA with various $g$; $a = 28.5\,\text{mm}$, $b = 28.5\,\text{mm}$, $d = 19.5\,\text{mm}$, $l_{feed} = 44\,\text{mm}$, $l = 15\,\text{mm}$, $w = 26\,\text{mm}$, $w_t = 20\,\text{mm}$, $w_b = 4\,\text{mm}$, $h_1 = 10\,\text{mm}$, $h_2 = 8\,\text{mm}$.

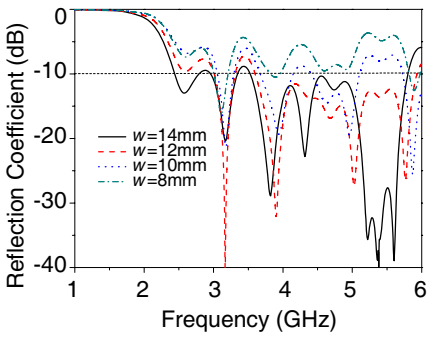


**Figure 4.** Reflection coefficient of various slot width $w$; $a = 28.5\,\text{mm}$, $b = 28.5\,\text{mm}$, $d = 19.5\,\text{mm}$, $g = 4\,\text{mm}$, $l_{feed} = 44\,\text{mm}$, $l = 15\,\text{mm}$, $w_t = 20\,\text{mm}$, $w_b = 4\,\text{mm}$, $h_1 = 10\,\text{mm}$, $h_2 = 8\,\text{mm}$.

frequencies of the DR increase with $g$ varying from 1 mm to 4 mm. This can be explained as a reducing effective permittivity of the hybrid structure [3]. For the second resonant mode, it can be found that, the center frequency of the second mode is almost unchanged. This property validates the idea that the second mode is defined by the isolated DR and is seldom affected by the air space. Table 1 lists the comparison of resonant frequency shift of the simulation and the modified formulas, respectively. It is also shown that, the resonant modes can be defined by using effective DR and isolated DR model.

**Table 1.** Simulated and calculated resonant modes.

| $g$ (mm) | $f_r$ (GHz) | | | | | | | |
|---|---|---|---|---|---|---|---|---|
| | $TE^{y}_{111}$ (effective) | | $TE^{y}_{111}$ (isolated) | | $TE^{y}_{113}$ (effective) | | $TE^{y}_{121}$ (isolated) | |
| | Simulated | Calculated | Simulated | Calculated | Simulated | Calculated | Simulated | Calculated |
| $g$=1 | 2.18 | 2.38 | 3.16 | 3.19 | 4.09 | 4.20 | 4.09 | 4.32 |
| $g$=2 | 2.39 | 2.43 | 3.16 | 3.19 | 3.96 | 4.18 | 4.20 | 4.32 |
| $g$=3 | 2.50 | 2.47 | 3.16 | 3.19 | 3.84 | 4.17 | 4.25 | 4.32 |
| $g$=4 | 2.58 | 2.52 | 3.17 | 3.19 | 3.75 | 4.16 | 4.29 | 4.32 |

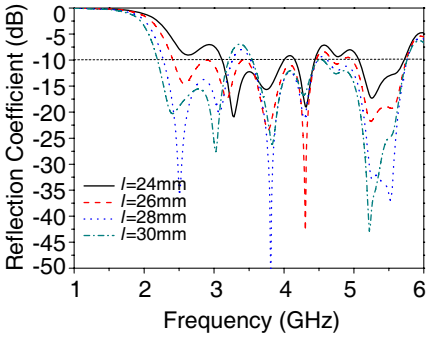


**Figure 5.** Reflection coefficient of various slot length $l$, $a$ = 28.5 mm, $b$ = 28.5 mm, $d$ = 19.5 mm, $g$ = 4 mm, $l_{feed}$ = 44 mm, $w$ = 26 mm, $w_t$ = 20 mm, $w_b$ = 4 mm, $h_1$ = 10 mm, $h_2$ = 8 mm.

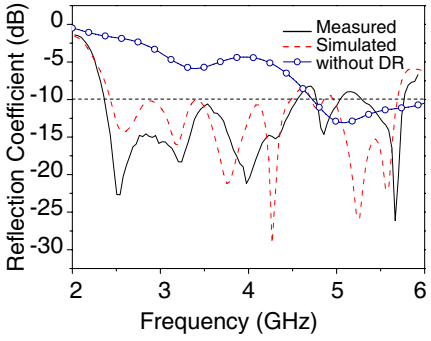


**Figure 6.** Measured and simulated reflection coefficient of the proposed DRA; $a$ = 28.5 mm, $b$ = 28.5 mm, $d$ = 19.5 mm, $g$ = 4 mm, $l_{feed}$ = 44 mm, $l$ = 15 mm, $w$ = 26 mm, $w_t$ = 20 mm, $w_b$ = 4 mm, $h_1$ = 10 mm, $h_2$ = 8 mm.

### 3.2. Effect of the Slot

To analyze the effects of the slot size, the parameter studies of the slot width $w$ and slot length $l$ were carried out. Fig. 4 shows the variation of the reflection coefficient against $w$. It is found that, the matching condition of the slot-DR is deteriorated with the decreasing slot width. However, since the back lobe will be enhanced due to the increasing slot width, the slot width should be chosen properly considering the matching bandwidth and acceptable back lobe. Fig. 5 shows the variation of the reflection coefficient against $l$. The matching

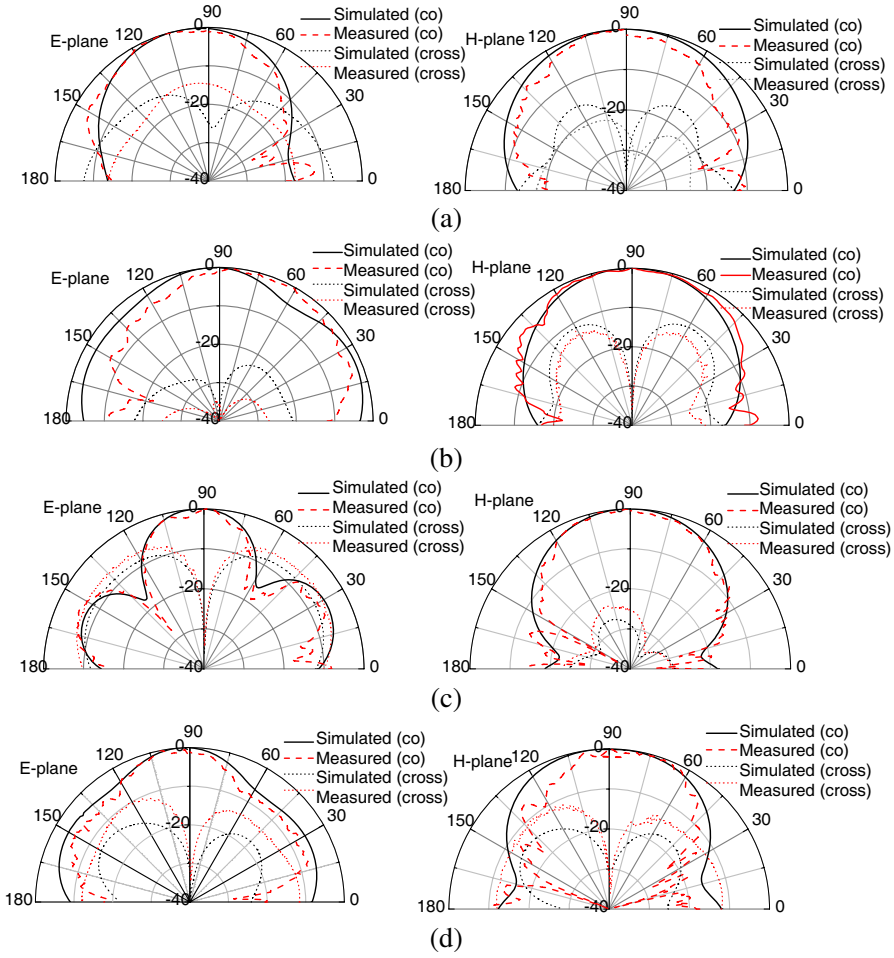


**Figure 7.** Measured and simulated radiation patterns of different resonant modes. (a) 2.6 GHz, (b)3.17 GHz, (c)3.7 GHz, (d)4.3 GHz.

of the first two modes is effected by the slot length. As a result, the slot size should be carefully designed to achieve a wide bandwidth.

## 4. EXPERIMENT RESULTS

To validate the proposed idea, one DRA is fabricated and measured. The DR size is selected as $a = 28.5\,\text{mm}$, $b = 28.5\,\text{mm}$ and $d = 19.5\,\text{mm}$. The optimized antenna parameters are chosen as follows: $g = 4\,\text{mm}$, $l_{feed} = 44\,\text{mm}$, $l = 15\,\text{mm}$, $w = 26\,\text{mm}$, $w_t = 20\,\text{mm}$, $w_b = 4\,\text{mm}$, $h_1 = 10\,\text{mm}$, $h_2 = 8\,\text{mm}$. The air gap is filled with foam with dielectric constant approximate equals 1. Fig. 6 shows the measured and simulated reflection coefficient results. A reasonable agreement between theoretical results and measured ones is observed. The impedance bandwidth of the proposed antenna covers the band width from 2.4 GHz to 4.5 GHz (10 dB reflection coefficient). The difference between the measured and simulated results may be due to the effects of the use of glue and fabrication errors. In addition, the simulated reflection coefficient for the antenna without dielectric resonator is also shown in Fig. 6 for comparison, demonstrating that a wider bandwidth is obtained by using a dielectric resonator. The proposed DR antenna was also measured in a far-field chamber. Fig. 7 depicts the measured radiation patterns at four frequencies. It is seen that the measured radiation patterns are symmetrical across the operating frequency range. The cross-polarization is acceptable comparing to convention antennas. Fig. 8 shows the peak gain of the proposed DRA. In the frequency range between 2.4 GHz and 2.8 GHz, the effective $TE^y_{111}$ mode is dominant, resulting in broadside operation with a gain around 7 dB. At around 3.2 GHz, the isolated $TE^y_{111}$ mode is excited, leading to a gain of 5–6 dB. The third mode is operating around 3.7 GHz with gain of 7 dB. The excitation of the fourth mode at 4.3 GHz results

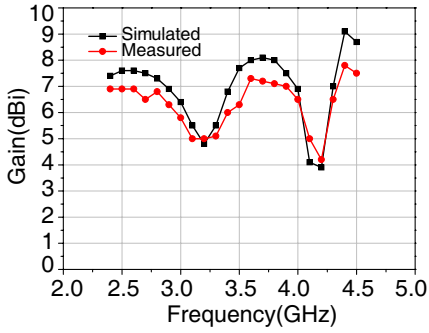


**Figure 8.** Measured and simulated peak gain of the proposed DRA.

in the rapid decrease of the broadside gain. Though there is some ripple of the gain, the proposed DRA can be a good candidate for the applications in various wideband communication systems.

## 5. CONCLUSION

In this paper, a dielectric resonator antenna has been investigated numerically and experimentally. The advantages of such a structure compared to conventional DRA are highlighted, and parametric studies have been carried out to optimize the antenna design. The results show that the bandwidth of the dielectric antenna can be greatly enhanced by properly exciting the DR. Finally, by using carefully designed feeding mechanism, a wideband DRA was proposed, exhibiting a simple but insightful design and impedance bandwidth exceeding 61%.

## REFERENCES

1. Shum, S. M. and K. M. Luk, "Stacked annular-ring dielectric resonator antenna excited by axi-symmetric coaxial probe," *IEEE Trans. Antennas Propagat.*, Vol. 43, 889–892, Aug. 1995.
2. Kishk, A. A., Y. Yin, and A. W. Glisson, "Conical dielectric resonator antennas for wide-band applications," *IEEE Trans. Antennas Propagat.*, Vol. 50, 469–474, Apr. 2002.
3. Walsh, A. G., S. D. Young, and S. A. Long, "An investigation of stacked and embedded cylindrical dielectric resonator antennas," *IEEE Antennas Wireless Propag. Lett.*, Vol. 5, 130–133, 2006.
4. Kishk, A. A., "Wide-band truncated tetrahedron dielectric sesonator antenna excited by a coaxial probe," *IEEE Trans. Antennas Propagat.*, Vol. 51, 2913–2917, Oct. 2003.
5. Denidni, T. A., Q. J. Rao, and A. R. Sebak, "Broadband L-shaped dielectric resonator antenna," *IEEE Antennas Wireless Propag. Lett.*, Vol. 4, 453–454, 2005.
6. Rao, Q. J., T. A. Denidni, and A. R. Sebak, "Broadband compact stacked T-shaped dra with equilateral-triangle cross sections," *IEEE Antennas Wireless Propag. Lett.*, Vol. 5, 130–133, 2006.
7. Petosa, A., N. Simons, R. Siushansiana, A. Ittipiboon, and M. Cuhaci, "Design and analysis of multisegment dielectric resonator antennas," *IEEE Trans. Antennas Propag.*, Vol. 48, 738–742, May 2000.
8. Coulibaly, Y., T. A. Denidni, and H. Boutayeb, "Broadband microstripfed dielectric resonator antenna for X-band applications," *IEEE Antennas Wireless Propag. Lett.*, Vol. 7, 341–345, 2008.

9. Kumar, A. V. P., V. Hamsakutty, J. Yohannan, and K. T. Mathew, "A wideband conical beam cylindrical dielectric resonator antenna," *IEEE Antennas Wireless Propag. Lett.*, Vol. 6, 15–17, 2007.
10. Liang, X. L., T. A. Denidni, and L. N. Zhang, "Wideband L-shaped dielectric resonator antenna with a conformal inverted-trapezoidal patch feed," *IEEE Trans. Antennas Propag.*, Vol. 57, 272–274, 2009.
11. Liang, X. L. and T. A. Denidni, "H-shaped dielectric resonator antenna for wideband applications," *IEEE Antennas Wireless Propag. Lett.*, Vol. 7, 163–166, 2008.
12. Mongia, R. K. and A. Ittipiboon, "Theoretical and experimental investigations on rectangular dielectric resonator antennas," *IEEE Trans. Antennas Propag.*, Vol. 45, No. 9, 1348–1356, Sep. 1997.
13. Zainud-Deen, S. H., H. A. El-Azem Malhat, and K. H. Awadalla "A single-feed cylindrical superquadric dielectric resonator antenna for circular polarization," *Progress In Electromagnetics Research*, Vol. 85, 409–424, 2008.
14. Abdulla, P. and A. Chakraborty, "Rectangular waveguide-fed hemispherical dielectric resonator antenna," *Progress In Electromagnetics Research*, Vol. 83, 225–244, 2008.
15. Al-Zoubi, A. S., A. A. Kishk, and A. W. Glisson, "Analysis and Design of a rectangular dielectric resonator antenna fed by dielectric image line through narrow slots," *Progress In Electromagnetics Research*, Vol. 77, 379–390, 2007.
16. Kishk, A. A., A. W. Glisson, and G. P. Junker, "Bandwidth enhancement for split cylindrical dielectric resonator antennas," *Progress In Electromagnetics Research*, Vol. 33, 97–118, 2001.
17. Rao, Q., T. A. Denidni, A. R. Sebak, and R. H. Johnston, "On improving impedance matching of a CPW fed low permittivity dielectric resonator antenna," *Progress In Electromagnetics Research*, Vol. 53, 21–29, 2005.
18. Junker, G. P., A. A. Kishk, A. W. Glisson, and D. Kajfez, "Effect of an air gap on a cylindrical dielectric resonator antennas operating in the TM01 mode," *Electronics Letters*, Vol. 30, No. 2, 97–98, 1994.
19. Ryu, K. S. and A. A. Kishk, "Ultra-Wide band dielectric resonator antenna with broadside patterns mounted on a vertical ground plane edge," *IEEE Trans. Antennas and Propagation*, Vol. 58, 1047–1053, Apr. 2010.